Chapter 6

Measurements

6.1 TRANSMITTANCE MEASUREMENTS IN FREE SPACE

The optical transmittance of the Fabry-Perot cavities fabricated in chapter 5 was first measured in a "free space". The measurement setup is shown in Figure 5.1. As a light source, a tungsten incandescent light was used. Since the spectral power density of the tungsten light is almost like that of a black body, a wide range of wavelengths can be obtained from this source. An excellent tunable light source was prepared by combining the lamp with a monochrometer, which was controlled by a programmable controller. Typical linewidth of the monochrometer was less than ±1 Å.

To monitor intensity fluctuations of the light source a beam splitter was used to direct part of the incident light beam to another photodetector. Also, an objective lens was used to focus the optical beam into the Fabry-Perot cavity, with lateral sizes in few hundred micron range. Transmitted intensity through the Fabry-Perot cavity was measured by a silicon p-n junction photodetector. For high signal-to-noise (S/N) ratio, a chopper was placed in front of the monochrometer and photocurrent signals at the photodetectors were fed into two lock-in amplifiers through transimpedance preamplifiers.

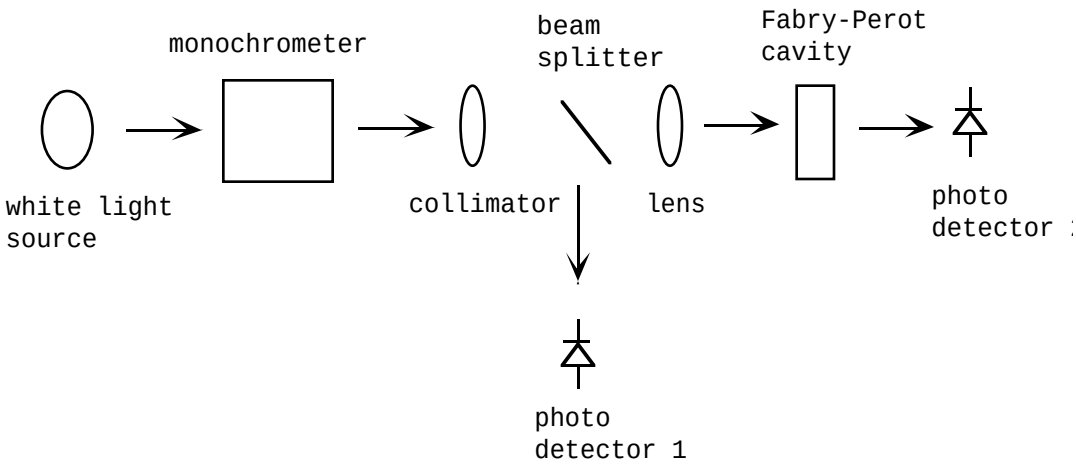

Figure 6.1 : Transmittance measurement setup in free space.

To compensate for the intensity fluctuation of the incident light, the intensities at the two photodetectors were measured simultaneously. However, it was observed that the spectral responsivities of the two photodetectors were different. To compensate for both the intensity fluctuation and discrepancy of the spectral responsivity of the photodetectors, two separate measurements should be performed. First, intensities of the light at the two photodetectors were measured without a Fabry-Perot cavity in front of photodetector 2 in Figure 6.1. Instead of the Fabry-Perot cavity, a pinhole, which has the same size as the cavity, was placed in front of photodetector 2. The measured intensity at photodetector 2 was used as a measure of the incident light intensity falling on the Fabry-Perot cavity and is called $RP2$. The intensity at photodetector 1 is called $RP1$. After the first

measurement, another measurement was performed with the Fabry-Perot cavity in front of photodetector 2. The intensities at the photodetectors during this measurement are called $DP1$ and $DP2$, respectively. Using the above measurements, the transmittance (T) of the Fabry-Perot cavity can be calculated as

$$T(\lambda) = \frac{DP2(\lambda)}{RP2(\lambda)} \cdot \frac{RP1(\lambda)}{DP1(\lambda)} \ . \tag{6.1}$$

The transmittance of the cavity was measured as a function of wavelength by changing the grating of the monochrometer. Figure 6.2 shows the measured transmittance of the Fabry-Perot cavity fabricated in chapter 5.

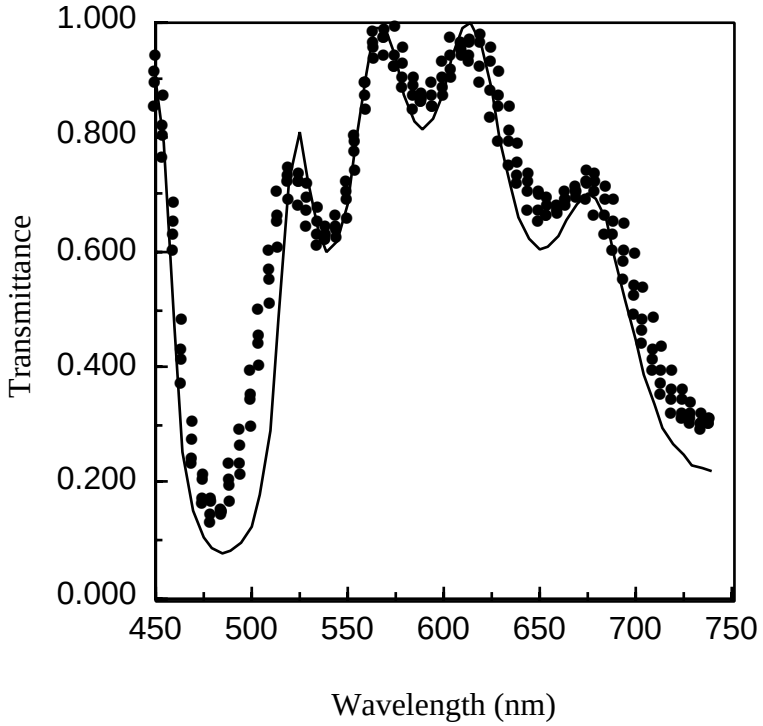

Figure 6.2 : Transmittance of a Fabry-Perot cavity with dielectric films mirrors and an air gap. Dotted line: measurement; solid line: simulation.

Transmittance of a Fabry-Perot cavity was measured four times independently. Figure 6.2 shows that each measurement was slightly different. The measurement error is believed to be caused by space-dependent intensity of the focused beam. It was verified using the pinhole that the focused beam had a space-dependent intensity. Since positioning the Fabry-Perot cavity at exactly the same location as the pinhole was very difficult, the actual incident intensity on the Fabry-Perot cavity was not exactly the same as the intensity with the pinhole. This resulted in slight variations for each transmittance measurement. However,

all the measured transmittances were still in good agreement with the simulated transmittance as shown in Figure 6.2. The transmittance of the Fabry-Perot cavity was calculated by using the characteristic matrix method as discussed in chapter 2. In the simulation, two 60 nm thick silicon nitride layers and a 420 nm thick silicon dioxide layer were used as the top mirror. As the bottom mirror, two 160 nm thick silicon nitride layers and a 450 nm thick silicon dioxide layer were used. And a 580 nm thick air gap was used.

6.2 PRESSURE MEASUREMENT IN FREE SPACE

We are now ready to measure differential pressure applied to the Fabry-Perot cavity by monitoring the transmittance of the cavity. Figure 6.3 shows a schematic view of a device holder which allowed the measurement of transmitted light intensity while applying pressure to the Fabry-Perot cavity. When differential pressure was applied to the cavity, the bottom diaphragm deflected and decreased the cavity gap. To verify the effect of a glass plate on the transmittance of the cavity, transmitted intensities with the glass plate were compared with one without the glass plate while the wavelength of the incident light was varied. Significant effect of the glass plate on the transmitted intensity was not observed.

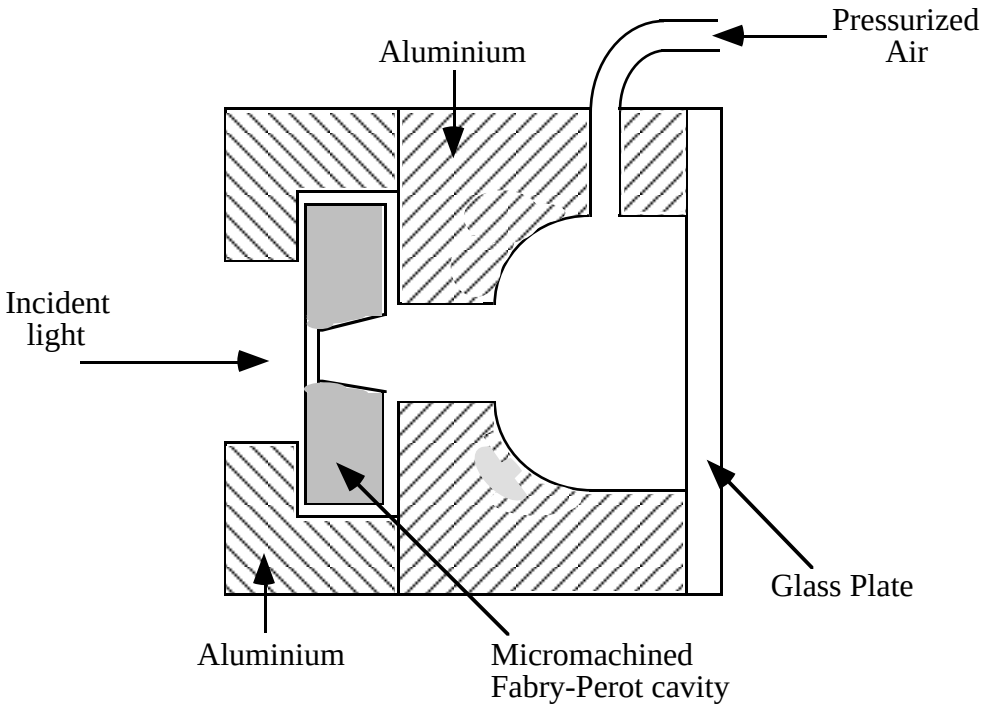

Figure 6.3 : Schematic view of a device holder for transmittance measurement. The holder allows measurement of transmitted light while applying pressure to a Fabry-Perot cavity.

The transmittance of the cavity was measured at various wavelengths as the pressure was varied. Figure 6.4 shows a plot of measured transmittance of the Fabry-Perot cavity as a function of differential pressure. In the figure, the transmittance at wavelengths of 630 and 450 nm are chosen for purposes of illustration. As expected, the transmittance of the cavity varies as the applied pressure increases. However, the amplitude of the transmittance curves are not as large as the curves predicted in chapter 2. Also, the transmittance curves do not have a period of one half the illumination wavelength.

The calculation done in chapter 2 assumed that the cavity gap changes uniformly over the whole optically illuminated region of the diaphragm when pressure is applied to the diaphragm. However, this assumption is not valid for the case where the bounday of a diaphragm is clamped and the diaphragm is illuminated over a large fraction of its area. Figure 6.5 illustrates the deflected shape of a square diaphragm for which the boundary is clamped. The Marcuse method was used to calculate the deflection, assuming no built-in stress in the diaphragm. The deflected shape leads to a significant variation in the amount of deflection over the optically sampled area, which is the whole surface of the bottom diaphragm in this case. However, the shape of the deflected diaphragm can be used to calculate an average transmittance.

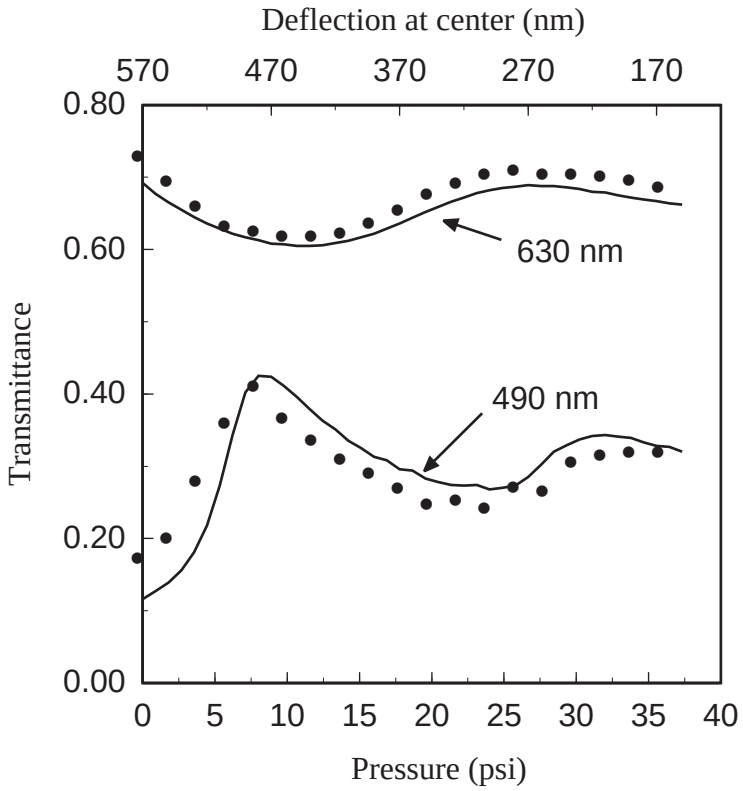

Figure 6.4: Transmittance of FP cavity; solid line: simulation; dotted line: measurement.

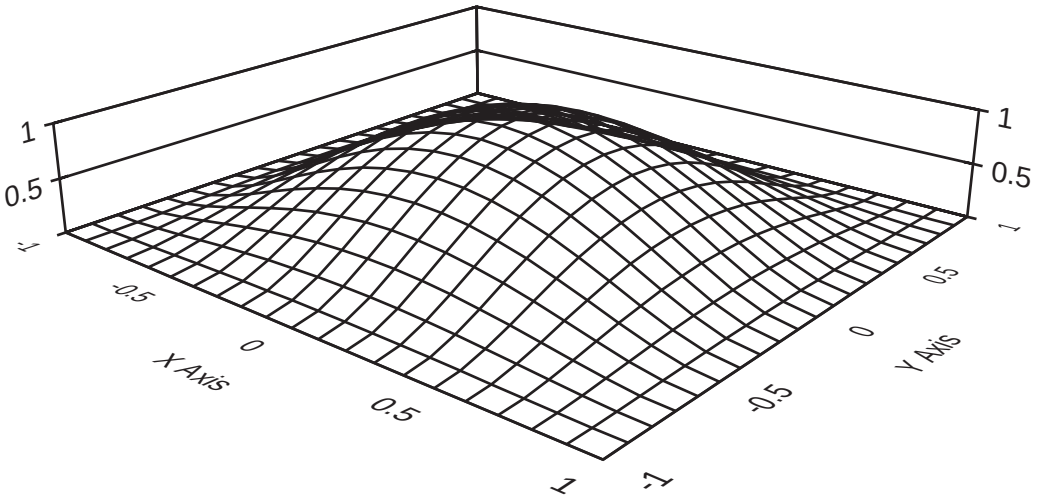

Figure 6.5 : Deflection of a square diaphragm without built-in stress. The deflection is normalized to the peak value.

First we will find the deflection and shape of the bottom diaphragm with clamped edges and built-in stress using the Marcuse method as described in chapter 4. To calculate the deflection of a diaphragm for a given pressure, the residual stress and Young's Modulus of the diaphragm must first be obtained. The equivalent residual stress and Young's Modulus of the bottom diaphragm were calculated using equation (3.1). The bottom diaphragm was assumed to have residual tensile stress of 0.3 GPa, as calculated from the residual stresses of the dielectric layers given in the section 4.1. The Young's Modulus of the diaphragm was assumed to be 170 GPa, as calculated using values from [1] .

For a bottom diaphragm $100 \times 100\ \mu m^2$ and 0.8 μm thick, the flexural rigidity D of the bottom diaphragm is calculated from

$$D = \frac{E \cdot h^3}{12 \cdot (1 - \upsilon^2)} = \frac{170GPa \times (0.8 \times 10^{-6})^3}{12(1 - 0.25^2)} = 7.74 \times 10^{-9}\ N/m^2.$$

As defined in the section 4.2, T_e of the bottom diaphragm is

$$T_e = 4\pi^2 D / a^2 \approx 30\ N/m.$$

The residual stress of the bottom diaphragm (0.3 GPa) is equal to $8T_e$. Using the values of D and T_e the deflection of the bottom diaphragm is calculated using the Marcuse method when differential pressure (q) is applied to the diaphragm. The equation for the deflection is

$$\omega = \frac{K}{236.7}\{1 - 0.219\cosh(2.556\xi) + 0.0002\cosh(8.51\xi)\} \times \{1 - 0.219\cosh(2.556\varphi) + 0.0002\cosh(8.51\varphi)\} \qquad (6.2)$$

where $K = \frac{a^4 \cdot q}{16D}$, $\xi = \frac{2x}{a}$, $\varphi = \frac{2y}{a}$, and a is length of the diaphragm. Note that the shape of the deflected diaphragm does not change even if applied pressure (q) increases. A contour map of the deflection is shown in Figure 6.6.

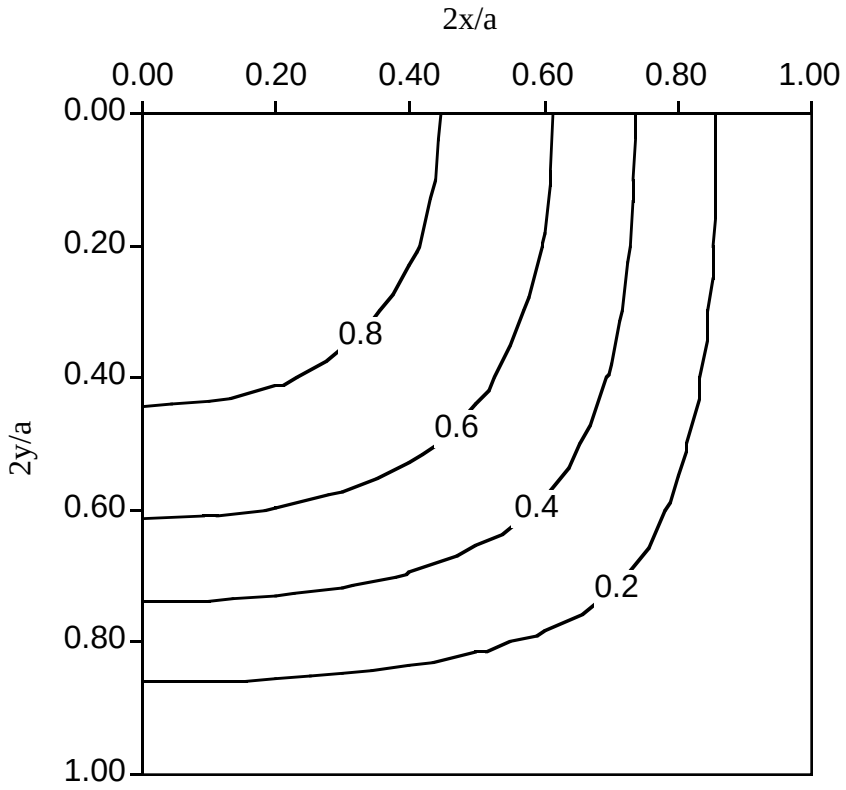

Figure 6.6 : Normalized deflection contour map of the bottom diaphragm with residual stress of 0.3 GPa.

The shape of the deflected diaphragm was used to find the fraction of the optically sampled area at each gap. A weighted average transmittance $\boldsymbol{T_{avg}}$ can then be calculated from

$$\boldsymbol{T_{avg}} = \frac{\sum [T(\boldsymbol{g}) \cdot A(\boldsymbol{g})]}{\sum A(\boldsymbol{g})} \tag{6.3}$$

where $T(\boldsymbol{g})$ is the reflectance of the cavity at gap $\boldsymbol{g}$ and $A(\boldsymbol{g})$ is the area with cavity gap $\boldsymbol{g}$.

To express the average transmittance as a function of applied pressure, the compliance of the bottom diaphragm should be calculated. The relationship between pressure and deflection at the center is obtained from equation (6.2)

$$\omega_{center} = \frac{q}{236.7} \cdot \frac{a^4}{16D} \cdot 0.61 \approx 130 \cdot q \ \ \text{Å} / psi. \tag{6.4}$$

For a given pressure, the deflection at the center can be calculated by equation (6.4); in turn the profile of the cavity gap over the whole area is calculated using equation (6.2). The average transmittance is then calculated using equation (6.3). The calculated average transmittance of the cavity is plotted as a function of pressure in Figure 6.4. The simulated curves agree quite well with the measured curves.

6.3 PRESSURE MEASUREMENTS USING OPTICAL FIBER INTERCONNECT

Remote pressure sensing was achieved by using a Fabry-Perot cavity fabricated in chapter 5 interconnected by an optical fiber. As a measurand, reflectance, instead of transmittance of the cavity, was used to sense changes in the cavity gap. This detection scheme will be very useful in practical applications where measurement of transmitted light is not allowed, for example the bearing application mentioned in chapter 1. Figure 6.7 shows a schematic diagram of the experimental setup.

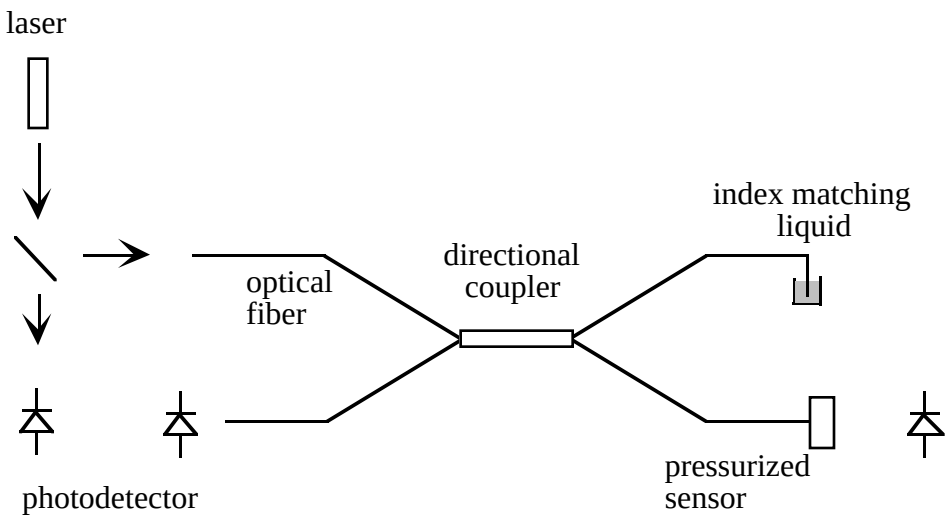

Figure 6.7 : Experimental setup for reflectance measurement with an optical fiber interconnect.

A 2×2 optical fiber directional coupler was used as an interconnect and a 633 nm He-Ne laser was used as a light source. The optical fiber consisted of a 100 μm diameter core and a 145 μm diameter cladding layer. For high signal-to-noise ratio a chopper and lock-in amplifiers were used as described in the last section. Also index matching liquid was used to avoid any reflected light at the end of the unused port of the directional coupler. The device holder shown in Figure 6.3 was used .

Figure 6.8 shows a view of the Fabry-Perot cavity coupled to an optical fiber. In the top view of the cavity, the boundary of the square bottom diaphragm is seen through the top mirror (Figure 6.8(a)). The optical fiber was aligned to the Fabry-Perot cavity using the guiding structure formed by anisotropic etching as shown in Figure 6.8(b). Since the diameter of the cladding layer is bigger that the width of the bottom diaphragm, there existed a few tens of micron space between the bottom mirror and the fiber when the fiber was inserted into the guiding structure at normal angle and finally contacted the (111) surface. The space prevents the deflected bottom diaphragm from touching the fiber. In this setup the cavity gap increases as a differential pressure is applied to the cavity. In contrast, the cavity gap would decrease when the die is flipped over in the jig.

In this configuration where the bottom diaphragm is deflected due to applied pressure, the maximum compliance of the bottom diaphragm is set by its maximum size, which is limited by the diameter of the fiber. For a more compliant diaphragm a cavity can be fabricated which has etch windows for the sacrificial layer in the bottom diaphragm. For such a cavity the top diaphragm will be deflected due to applied pressure, and the compliance of the diaphragm is not limited by the size of the fiber, but set by the size of the pre-patterned sacrificial layer.

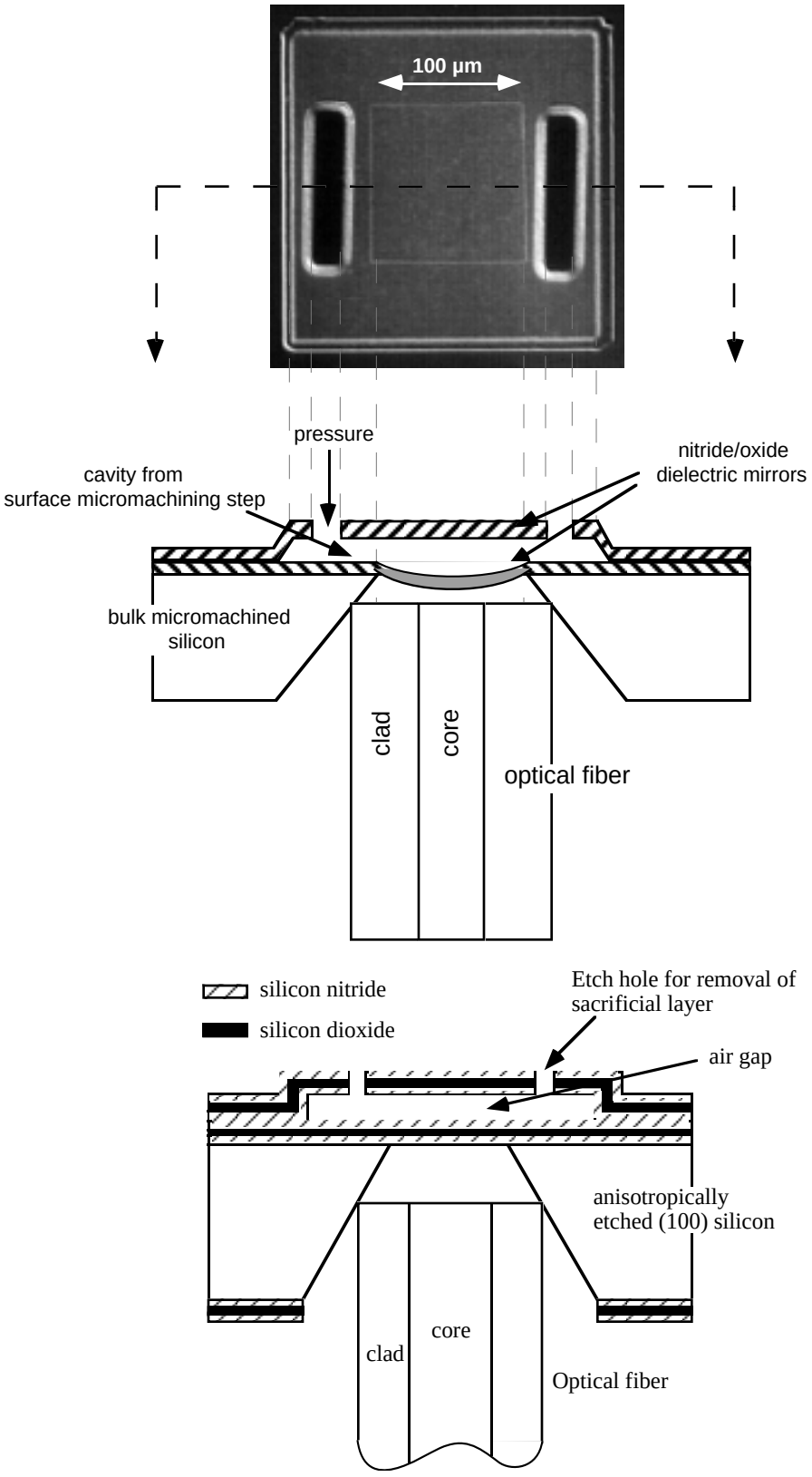

Figure 6.8 : View of a Fabry-Perot cavity coupled to an optical fiber.
(a) photograph of top view of the cavity ; (b) cross section of the cavity coupled to an optical fiber.

The reflectance of the cavity was measured as a function of pressure. The measurement procedure was the same as the one for transmittance described in the last section. Transmitted and reflected intensities were measured at the same time. Figure 6.9 shows transmittance and reflectance of the Fabry-Perot cavity measured at the end of the fiber.

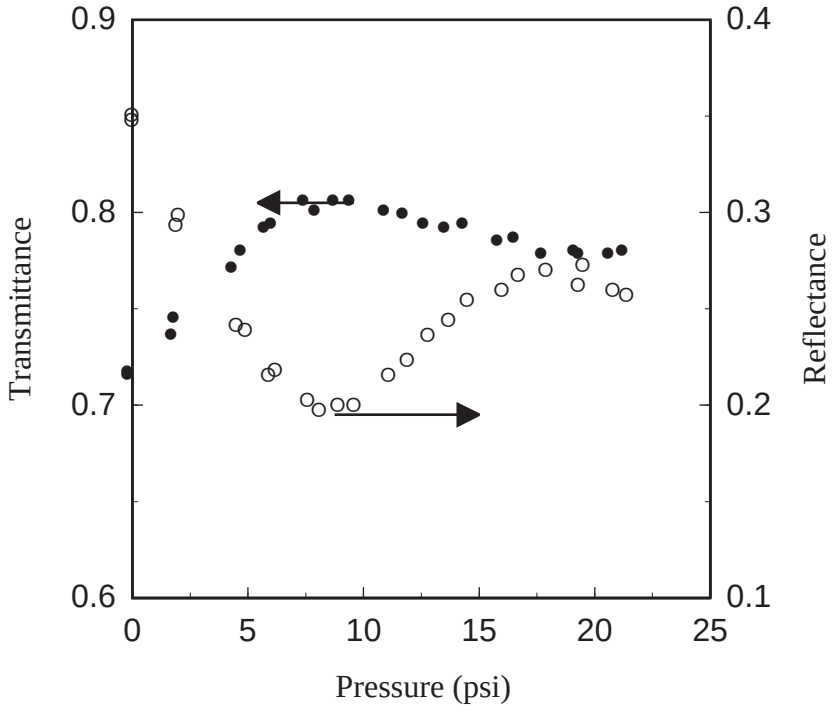

Figure 6.9 : Measurement of reflectance and transmittance of the Fabry-Perot cavity coupled to an optical fiber. Black dot: Transmittance; open dot: Reflectance.

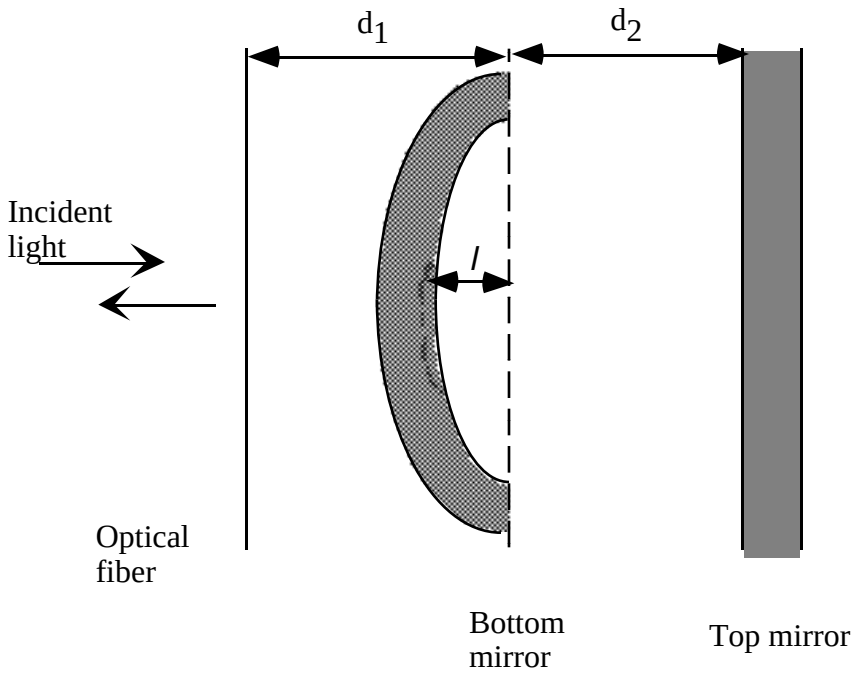

Figure 6.10 : A model for a Fabry-Perot cavity coupled to an optical fiber. A deflection of the bottom diaphragm causes changes in both d_1 and d_2, simultaneously.

When the cavity is coupled to the fiber as shown in Figure 6.8, the structure can be modeled by a cavity with two air gaps as shown in Figure 6.10. The characteristic matrix, corresponding to the gap between the fiber and the bottom mirror, was added to the product of the characteristic matrices corresponding to the micromachined cavity. Note that a deflection of the bottom diaphragm would cause changes in the two air gaps (d_1 and d_2) simultaneously as shown in Figure 6.10 . The reflectance of the cavity was calculated as a function of gap (d_2) using a normal incident plane wave approximation. Average

transmittance was calculated using equation (6.3). The initial thickness of the space (d_1) was adjusted as a fitting parameter to match the measured reflectance, shown in Figure 6.11.

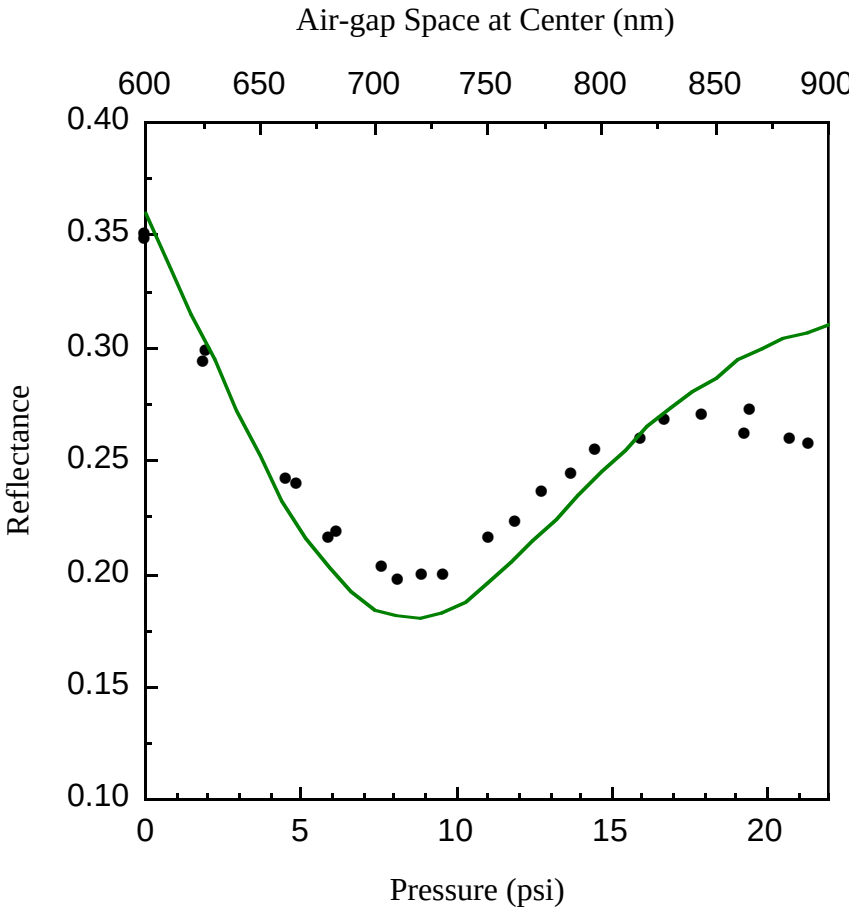

Figure 6.11 : Reflectance of a Fabry-Perot sensor as a function of applied pressure. Solid line: simulation ; dotted line: measurement.

6.4 SUMMARY

Fabry-Perot cavities fabricated in chapter 5 were demonstrated as a pressure sensor. The pressure measurement was performed by using the micromachined Fabry-Perot cavity and an optical fiber as an interconnect. The measured optical response of the cavity was in good agreement with simulation, which took into account the shape of a deflected diaphragm and the mechanical compliance of the diaphragm. It was also shown that even in the case where a Fabry-Perot cavity is coupled to a multimode optical fiber, the optical response of the cavity could be approximated by using a normal incident plane wave model.